Environmental Science & Technology

Article

pubs.acs.org/est

Role of Pb(II) Defects in the Mechanism of Dissolution of Plattnerite (β-PbO_2) in Water under Depleting Chlorine Conditions

Daoping Guo, Clare Robinson, and Jose E. Herrera*

Department of Civil and Environmental Engineering, Western University, London, Ontario, Canada N6A 5B9

Supporting Information

ABSTRACT: Destabilization of lead corrosion scales present in plumbing materials used in water distribution systems results in elevated lead concentrations in drinking water. Soluble lead release caused by changes in water chemistry has been linked to dissolution of lead carbonate and/or lead oxide solid phases. Although prior studies have examined the effects of varying water chemistry on the dissolution of plattnerite (β-PbO_2), β-PbO_2 dissolution under depleting chlorine conditions is poorly understood. This paper reports results obtained for long-term batch dissolution experiments for solid phase β-PbO_2 under depleting chlorine conditions. Results indicate that the initial availability of free chlorine effectively depresses dissolved lead concentrations released from β-PbO_2. However, the dissolved lead levels remained low (~4 μg/L) even after free chlorine was depleted. Detailed spectroscopic characterization of solid samples collected during the β-PbO_2 experiments indicates that changes in the electronic structure of PbO_2 occurred during the dissolution. This further points out that Pb^{2+} defects present in crystalline β-PbO_2 play a dominant role in the dissolution of this solid phase.

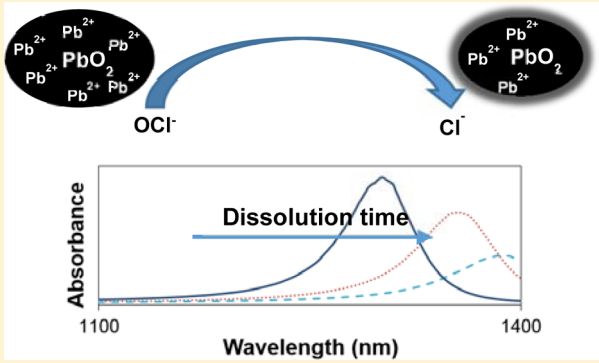

INTRODUCTION

PbO_2 is often found in corrosion scales of lead-bearing plumbing in drinking water distribution systems (DWDS). Tetragonal plattnerite (β-PbO_2) and orthorhombic scrutinyite (α-PbO_2) are both generally observed in the surface layer of corrosion scales as dissolved[1−4] and solid lead(II) species[5−9] are oxidized by free chlorine to form these PbO_2 phases. It is well recognized that the stability of PbO_2 can significantly affect dissolved lead levels in drinking water.[1] Many studies have examined the effects of water quality parameters such as pH, dissolved inorganic carbon (DIC), and disinfectant type on PbO_2 stability, together with the effect of reductants naturally present in drinking water such as Fe^{2+} and natural organic matter (NOM).[10−15]

PbO_2 is less soluble than solid lead(II) carbonates ($PbCO_3$ and $Pb_3(OH)_2(CO_3)_2$) according to tabulated thermodynamic data and previously reported experimental results.[1,16] PbO_2 is generally stable when high oxidation−reduction potential (ORP) is maintained in a DWDS by free chlorine. However, a decrease in ORP due to, for example, a change in disinfectant, may destabilize PbO_2 and cause dissolved lead concentrations to rapidly increase. This was observed in Washington, DC, USA, when the disinfectant was switched from free chlorine to chloramine.[17−19] Understanding PbO_2 dissolution under depleting chlorine, and thus decreasing ORP conditions, is essential to evaluate and predict lead levels in drinking water and for developing effective long-term corrosion control strategies. However, only a few studies[10,20] have examined this scenario, and the long-term solid phase transformations and subsequent dissolved lead concentrations in drinking water have not been comprehensively investigated under depleting chlorine conditions.

β-PbO_2 is thermodynamically more stable in chlorinated water with relatively low pH levels (8−10) than α-PbO_2.[5,7,20−22] For most DWDS, drinking water is slightly basic, suggesting β-PbO_2 formation is favored. The objective of this work was to understand the fundamental physicochemical processes governing β-PbO_2 dissolution in water under depleting chlorine conditions and the influence of free chlorine concentrations on the dissolution of β-PbO_2. With this purpose, long-term batch β-PbO_2 dissolution experiments were carried out. Characterization of solid samples collected during these experiments provides important insights into the β-PbO_2 dissolution mechanisms. Relatively high initial concentrations of free chlorine (up to 5 mg Cl_2/L) were used in experiments to completely oxidize the labile surface of PbO_2 and provide sufficient oxidant for the characterization of structural changes.

EXPERIMENTAL SECTION

Materials. β-PbO_2 (Sigma-Aldrich) was used without further purification for the dissolution experiments. The average particle size of the β-PbO_2 solid is 27.1 μm as

Received: April 30, 2014
Revised: August 18, 2014
Accepted: August 19, 2014
Published: August 19, 2014

dx.doi.org/10.1021/es502133k | Environ. Sci. Technol. 2014, 48, 12525−12532

determined via dynamic light scattering (Mastersizer 2000). NaOCl (Fisher Scientific, 5.65−6% w/w, laboratory grade) was used as the source of free chlorine. $NaNO_3$ (Sigma-Aldrich, ≥99.0%) and $NaHCO_3$ (Sigma-Aldrich, ≥99.5%) were used to prepare a stock solution with 0.01 M ionic strength and 20 mg C/L dissolved inorganic carbon (DIC), respectively. NaOH (pellets, Sigma-Aldrich) and 67−70% v/v condensed HNO_3 (EMD Milipore, Omnitrace) were used to prepare 0.1 M NaOH and 0.1 M HNO_3 solutions, respectively. All solutions were prepared using megapure water and ACS reagent grade chemicals except for the NaOCl solution.

β-PbO_2 Batch Dissolution Experiments. Batch experiments were carried out to evaluate the lead release profile and solid phase transformation during dissolution process via aqueous and solid phase analysis. Detailed experimental conditions of each experiment are described in the Supporting Information (SI). All experiments were performed at 0.88 g/L solid concentration and in a closed system configuration with no head space [0.01 M ionic strength, 20 mg C/L DIC, and target initial free chlorine concentrations (2.5 and 5.0 mg/L as Cl_2) at an initial pH value close to 8 (unbuffered)] to avoid carbonate exchange with air. All vials were put in a sealed dark box to avoid light-induced degradation of free chlorine and continuously mixed on a shaker (Thermo Scientific, MAXQ 2000) at 170 rpm. Control test was performed as well with duplicate samples under the same conditions but in the absence of free chlorine. Sacrificial samples were collected regularly for each time series data point. Samples were pressure filtered using a 0.22 μm poly(ether sulfone) (PES) syringe filter (VWR) using a 10 mL syringe (Discovery Labware) to measure free chlorine, ORP, and pH values. For each sample, the first few drops of the filtrate were discarded. One milliliter of 20% nitric acid was added to a 10 mL aliquot of filtrate for ICP-OES or ICP-MS analysis. Solid samples were collected, dried, and stored in a vacuumed desiccator. This same sampling procedure was used for the control test, with the exception of the measurement of free chlorine. All experiments were conducted at room temperature (21 ± 2 °C).

Analysis Methods. Dissolved lead concentrations were determined via inductively coupled plasma optical emission spectrometry (ICP-OES) (Varian, Vista-Pro Axial) and inductively coupled plasma mass spectrometry (ICP-MS) (Agilent, 7500cx). The pH value was measured after filtration with a nonglass ISFET probe and pH meter (Hach, H160), which is calibrated by using a three-point method [pH 4, 7, and 10 (BDH)]. ORP was measured using a glass ORP probe. Freshly prepared quinhydrone buffer solutions at pH 4 and 7 were used for calibration of the probe. The ORP values are reported against the standard hydrogen electrode (vs SHE) by adding 210 mV into measured results as per the manufacturer's instruction. The concentration of free chlorine was measured using the standard DPD colorimetric method (method 10069, Hach) in an UV/vis spectrophotometer (Hach, DR5000).

Solid samples were characterized by ultraviolet/visible/near-infrared (UV/vis/NIR) spectroscopy using an UV-3600 Shimadzu equipped with a Praying Mantis. The spectra were obtained in diffuse reflectance mode over the range from 200 to 1400 nm with 1 nm step size using the highest resolution setting of the instrument. For the case of PbO_2 solids the NIR spectra (1100−1500 nm) results from electronic transitions from the valence band to the conduction band as the energy of the photons matches the band gap energy in the solid. The position of the band is thus related to the electronic structure of the PbO_2 solid. This technique has been widely used for probing lead oxide bearing semiconductors as it directly probes the electronic structure of these solids. Raman spectra on the solid samples were obtained in a Jovin Yvon-Horiba LabRam 800 (air-cooled CCD detector) with a He−Ne laser (632.8 nm) tuned at 610 μW to avoid sample decomposition. The X-ray diffraction (XRD) patterns were obtained on a Rigaku RPT 300 RC diffractometer using Co Kα (λ = 1.78890 Å) radiation over the range of 10−70° 2θ with a 0.02° step size.

RESULTS AND DISCUSSTION

Influence of Free Chlorine on Lead Release Profile and Equilibrium Concentrations. The free chlorine and lead concentrations observed during experiments with nominal initial free chlorine concentration of 2.5 mg/L as Cl_2 are shown in Figure 1. The free chlorine concentration decreased

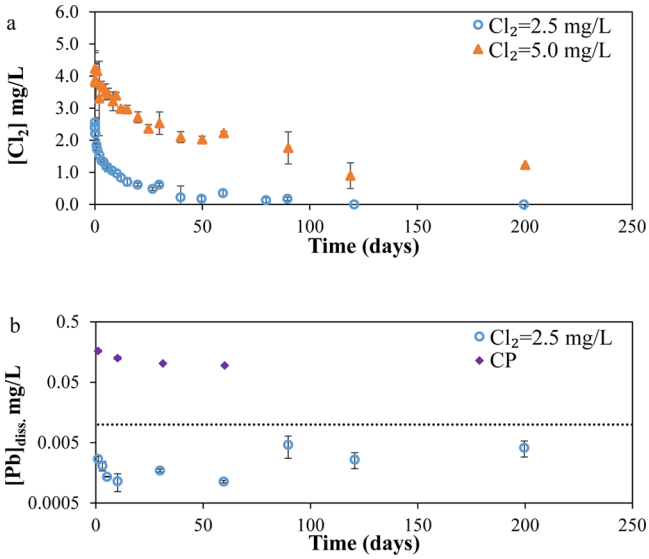

Figure 1. (a) Free chlorine consumption profile and (b) dissolved lead concentrations observed during β-PbO_2 dissolution experiments at two different initial free chlorine concentrations and in a control test (CP). The dashed line represents the maximum lead concentration (MAC) of 10 μg/L.

exponentially over time-; during the first 10 days, the free chlorine decreased rapidly from 2.5 to 1.0 mg/L, followed by a decrease to 0.1 mg/L at 80 days and complete consumption by 120 days. The dissolved lead concentrations remained relatively constant during the experiment, although a slight increase in concentration was observed (~0.004 mg/L) at 90 days even though free chlorine was still available (~0.1 mg/L) and the ORP was approximately 660 mV (SI Figure S1a). This is consistent with the fact that there is a threshold value of free chlorine concentration needed for PbO_2 formation. During the first 90 days free chlorine likely oxidized the dissolved lead species ($Pb^{2+}_{(aq)}$) released from the reduction of β-PbO_2 by water (eq 1).[7,17,18,20] This results in the reprecipitation of PbO_2 and consumption of free chlorine (eq 2). The pH levels remained relatively stable at 8.1 ± 0.2 throughout the experiments (SI Figure S1b).

$$PbO_{2(s)} + H_2O_{(l)} \leftrightarrow Pb^{2+}_{(aq)} + 2OH^-_{(aq)} + 0.5O_{2(aq)} \quad (1)$$

dx.doi.org/10.1021/es502133k | Environ. Sci. Technol. 2014, 48, 12525−12532

$$Pb^{2+}_{(aq)} + OCl^{-}_{(aq)} + H_2O_{(l)} \leftrightarrow Cl^{-}_{(aq)} + PbO_{2(s)} + 2H^{+}_{(aq)} \quad (2)$$

The lead levels observed in experiment using a nominal initial chlorine concentration of 2.5 mg/L during the first 90 days under depleting chlorine conditions are similar to those previously reported.[10,15,23] However, dissolved lead concentrations remained low (~0.004 mg/L) after 90 days and up to the end of the experiments (200 days), even though free chlorine was completely depleted at 120 days. Contrasting these results, much higher dissolved lead concentrations (~0.1 mg/L) were observed in a control experiment conducted with no free chlorine (Figure 1b). The low final dissolved lead levels observed in our experiments after chlorine was fully depleted were unexpected. Previous studies[10,24] reported lead concentrations as high as 0.05 mg/L during β-PbO_2 batch dissolution experiments with no free chlorine. Our control experiment (no chlorine) also suggests that high dissolved lead concentrations should be observed in the absence of chlorine. The ORP values observed at 200 days were about 360 mV—lower than those obtained in the control experiment (no chlorine) (~610 mV) (SI Figure S1a). The observed low lead concentrations at low ORPs suggest that once chlorine is depleted, the prevailing ORP is not the critical factor controlling the dissolution of β-PbO_2 in our system. This result is consistent with prior batch studies[15,24] linking high dissolved lead concentrations to the decay of disinfectant but not to ORP changes. However, by comparison with our control test results, it is evident that the prior availability of chlorine does play a determinant role in the long-term β-PbO_2 stability.

Redox potential measurements have been widely used in the geochemical field and had been applied in the study of some drinking water systems.[25,26] Although redox potential is potentially a good descriptor of water quality, its measurement and interpretation of resulting values are difficult as some limitations are imposed by the electrodes used and even the sample matrix.[27,28] The Pt-electrodes, commonly used for their high exchange current density, sometimes develop an oxidation layer on their surface, delaying response time if the sample contains high concentrations of oxygen or oxidants.[29] For instance, Copeland and Lytle[25] observed probe contamination and/or precipitate formation during ORP measurements for oxidants in drinking water. We performed regular electrode cleaning and maintenance trying to avoid the formation of the oxidation layer and did not observe precipitate formation during the experiments. Because neither bromide nor sulfide ions were present in solution, there is no potential for poisoning the ORP electrode. However, it is still difficult to avoid variations in the measurements even though these precautions are taken. We consistently used the same electrode to obtain ORP values and obtained relatively low standard deviations during measurements (<20 mV).

To the best of our knowledge, our experiments are the first to report low dissolved lead levels for β-PbO_2 dissolution after chlorine is completely consumed. To better understand these observations, we carried out a detailed characterization of the solid phase transformations occurring during dissolution.

Solid Phase Characterization. *NIR Spectroscopy.* Figure 2 shows the NIR spectra obtained for the β-PbO_2 solid phase before dissolution and for solid samples collected during dissolution at 10 and 90 days for the experiment conducted using 2.5 mg/L as initial Cl_2. A clear peak is observed in the 1200−1400 nm range. Table 1 shows the position of this NIR peak for all solid samples collected during experiments with nominal initial free chlorine concentrations of 2.5 and 5.0 mg/L as well as the samples of control test (no chlorine). The full spectra are shown in Figure S2 (SI). The NIR peak is observed for all solid samples collected during dissolution, but the position of the peak shifted to longer wavelengths as dissolution time increased for the experiments run in the presence of chlorine. Moreover, the shift of the NIR peak (in nm) with time closely followed the consumption of free chlorine in the system (SI Figure S3). This suggests that changes in the morphology of β-PbO_2 observed via the NIR peak shift are linked to the consumption of chlorine. In contrast to these observations, for the samples collected during the control experiment (no chlorine), a general shift of the peak to shorter wavelengths was observed (Table 1 and SI Figure S4).

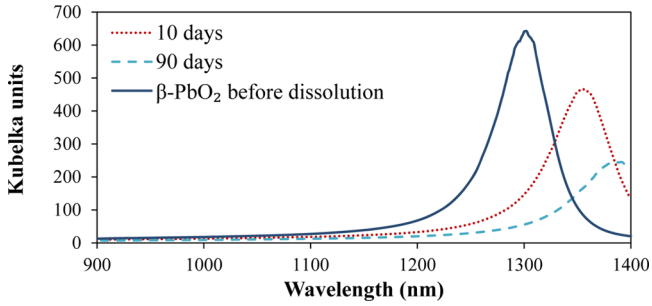

Figure 2. NIR spectra of solids collected during experiment with a nominal initial free chlorine concentration of 2.5 mg Cl_2/L.

Table 1. NIR Peak Position of Solid Samples Collected from Dissolution Experiments with Nominal Initial Free Chlorine Concentrations of 2.5 and 5.0 mg/L and from the Control Test (No Chlorine) over Time

	peak position (nm)		
time (days)	Cl_2 = 2.5 mg/L	Cl_2 = 5.0 mg/L	control test (Cl_2 = 0 mg/L)
0	1300	1296	1299
10	1356	1335	1285
30	1380	1347	1298
60	1348	1389	1308
90	1383	N/A	N/A

To fully grasp the significance of these results, it is necessary to understand the spectroscopic origin of the NIR peak. The NIR peak observed for PbO_2 species is linked to an electronic transition in the band gap present in these solids. Features in the electronic spectra of lead oxides have been well studied in the field of lead-containing thin films and glasses often used in optical technology and, more recently, for the development of transparent conducting materials.[30−36] From these prior studies, the peak observed in the NIR spectra of PbO_2 can be rationalized in terms of a symmetry-forbidden electronic transition from the upper valence band into the solid's conduction band.[34,35] The band gap is defined as the energy difference between the upper valence band and lower conduction band in the solid phase. Keester and White[36] obtained a linear correlation between band edge calculated from the optical spectra of solid lead oxides and the average oxidation state, suggesting that the NIR feature observed in PbO_2 species arises from small amounts of Pb^{2+} present in the

β and α forms of PbO_2. Since this seminal work, much progress[33−35] has been made in understanding these spectroscopic features. Whereas the electronic structures of PbO and Pb_3O_4 are now relatively well understood, the band structure of PbO_2 is still controversial. It has however been established that the NIR peak arises due to the presence of Pb^{2+} defects in PbO_2, which result in charge compensation occurring through electrons in the PbO_2 conduction band.[34,37]

Using the work by Keester and White[36] as a starting point, we attempted to link the average Pb oxidation state in lead oxides to the band gap energies calculated from the UV/vis/NIR spectra obtained for solid phase PbO, Pb_3O_4, and both α- and β-PbO_2. The band gap energy (E_g) was calculated using the well-known Davis and Mott[38] model, which relates the absorption coefficient (α) to the photon energy ($h\nu$) for various electronic transitions prevalent in semiconductors. In this model

$$(h\nu\alpha)^{1/n} = A(h\nu - E_g) \quad (3)$$

where h is Planck's constant, ν is the radiation frequency, A is a proportionality constant, and n describes the electronic transition type, taking values of 1/2, 3/2, 2, or 3, depending on the type of transition: direct allowed, direct forbidden, indirect allowed, and indirect forbidden, respectively. When diffuse reluctance spectra are used to calculate the band gap, eq 3 becomes

$$(h\nu F(R))^{1/n} = A(h\nu - E_g) \quad (4)$$

where $F(R)$ is the Kubelka−Munk function quantifying light absorption for the solid. Although prior studies described above indicate that the type of electronic transition observed in PbO_2 is likely to be indirect forbidden, the exact mechanism is uncertain. It is common practice to select the n value on the basis of the best linear fit of the band gap edge region in the spectra.[39,40] Thus, to select the value for n, all four values (1/2, 3/2, 2, and 3) were tested and used to plot $(h\nu F(R))^{1/n}$ against $h\nu$ for lead oxide phases (PbO, Pb_3O_4, α- and β-PbO_2). We determined that n = 1/2 gave the best linear fit for the edge absorption region. Thus, we used the power of 2 of the Kubelka−Munk function multiplied by the photon energy in eq 4, which provides the edge energy value after extrapolation to zero absorbance for amorphous semiconductors. We also performed this calculation for $Pb_{12}O_{19}$ and Pb_2O_3 after digitalizing the data originally reported for these solids by Keester and White.[36] The linear correlation we obtained between average Pb oxidation state and calculated average band gap energy is shown in Figure 3 for the solid phases PbO, Pb_3O_4, $Pb_{12}O_{19}$, and Pb_2O_3.

As mentioned above, it is well acknowledged that the NIR spectrum peak (~1300 nm) is linked to the presence of Pb^{2+} defects in the PbO_2 crystalline structure. Thus, we used the data shown in Figure 3 to extrapolate the expected band gap energy for a perfect (100% of lead species as Pb^{4+}) PbO_2 solid. Using the same correlation, we calculated the apparent number of Pb^{2+} defects (in percentage of [Pb^{2+}]/[total Pb]) present in both β-PbO_2 and α-PbO_2 solids on the basis of their calculated gap energies obtained from their NIR spectra. This calculation suggested values of 9.4 and 6.8% of Pb^{2+} present in these solids, respectively (Table 2). Despite the uncertainty of band gap (<0.6%) generated by the spectral resolution of the optical absorption data, this approach provides an upper limit reference for the number of defects present in the PbO_2 sample.

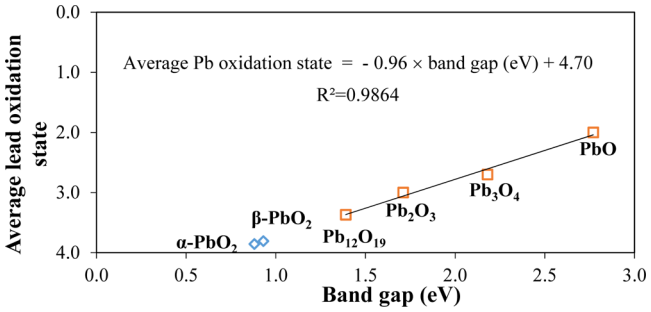

Figure 3. Correlation between average lead oxidation state and band gap edge energy obtained using β-PbO, Pb_3O_4, $Pb_{12}O_{19}$, and Pb_2O_3. The experimental values obtained for β-PbO_2 (before dissolution) and α-PbO_2 are also shown.

Table 2. Band Gap Energy and Lead Oxidation State of PbO, Pb_3O_4, Pb_2O_3, $Pb_{12}O_{16}$, α-PbO_2, and β-PbO_2 as well as Nominal Percentage of Pb(II) and Pb(IV) Present in These Lead Oxides[a]

		Pb oxidation state			
	band gap (eV)	average	predicted	Pb(II) (%)	Pb(IV) (%)
PbO	2.77 ± 0.007	2		100	0
Pb_3O_4	2.21 ± 0.008	2.7		65	35
Pb_2O_3	1.71	3		50	50
$Pb_{12}O_{19}$	1.39	3.37		31	69
α-PbO_2	0.88 ± 0.002	4 (nominal)	3.86	6.8	93.2
β-PbO_2	0.93 ± 0.004	4 (nominal)	3.81	9.4	90.6

[a]Data for β-PbO_2 were obtained before dissolution experiments.

Moreover, the values we obtained for the apparent number of Pb^{2+} defects are within the same order of magnitude as those reported by Scanlon et al.[34] for crystalline β-PbO_2 using neutron diffraction.

From this analysis the changes in the NIR spectra shown in Figure S2 (SI) can be linked to the oxidation of Pb^{2+} defects in the PbO_2 lattice by free chlorine. In contrast, the shift to shorter wavelengths observed in the control experiment (no chlorine) suggests the formation of additional Pb^{2+} moieties, likely the result of PbO_2 reduction by water.[14,15,41] If a similar approach as the one described above, which relates the calculated band gap to the number of Pb^{2+} defects in the reference lead oxides, is applied to the spectra of the solids collected during experiments with initial free chlorine, a profile describing the amount of Pb^{4+} over time can be obtained. This plot is shown in Figure 4. It can be seen that the percentage of Pb^{4+} species present in the solid increases over time, following the profile for chlorine consumption. This increase in Pb^{4+} species is dependent on the amount of free chlorine consumed, but not of the absolute value of initial chlorine concentrations. In other words, the larger the amount of free chlorine consumed, the higher the percentage of Pb^{4+} observed in PbO_2. However, there is no direct quantitative relationship between the amount of Pb^{4+} present in PbO_2 and free chlorine consumed because chlorine is also consumed to reoxidize dissolved lead(II) ions (eqs 1 and 2). The bathochromic shift in the NIR band is therefore caused by a decrease in the amount of Pb^{2+} defects in PbO_2 by oxidation. This is in agreement with Izvozchikov,[42] who showed experimentally that the band gap energy value decreases as the oxidation state of Pb increases. It should be noted that the NIR peak does not shift back to its original

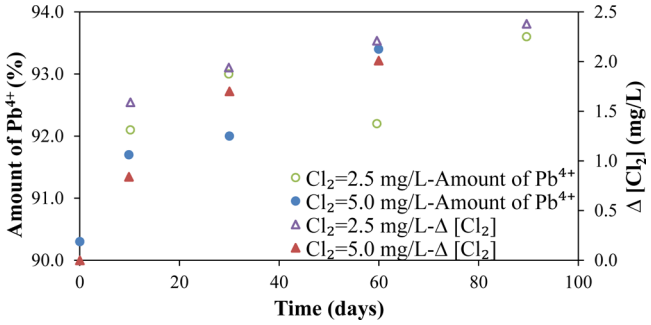

Figure 4. Correlation between the percentages of lead atoms present as Pb^{4+} in PbO_2 obtained from the NIR band edge energy calculation and the consumption of free chlorine during dissolution over time.

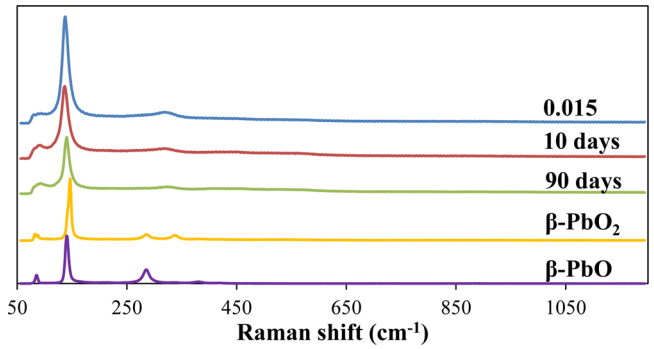

Figure 5. Raman spectra obtained on the solids collected during dissolution experiment with a nominal initial free chlorine concentration of 5.0 mg Cl_2/L.

position even though the free chlorine level was lower than the threshold value for PbO_2 formation.[7] This observation indicates that the newly generated Pb^{4+} sites remain within the β-PbO_2 crystal lattice. In addition, the electronic transition linked to the NIR peak occurs between well-defined electronic bands in the solid. In other words, the Pb^{2+} defects should be part of the lattice such that they affect the electronic band structure of the solid. Therefore, we can propose that the NIR peak shift is not caused by oxidation of adsorbed Pb^{2+} as adsorbed species will not affect the electronic structure of the solid lattice. Furthermore, we can hypothesize that the new form of crystalline PbO_2 oxidized by free chlorine with fewer Pb^{2+} defects has a more stable crystalline/electronic structure toward dissolution than the initial β-PbO_2 phase in our system. The formation of a more stable structure explains why low final dissolved lead concentrations were observed even when chlorine was completely consumed and the ORP levels were low.

Raman Spectroscopy. To correlate the observed NIR peak shift and associated band gap changes with morphological changes to β-PbO_2 that may have taken place during dissolution, we carried vibrational spectroscopy analysis on the samples. β-PbO_2 has Raman-allowed transitions but with extremely low cross sections.[43−45] We characterized solid samples collected for the experiment using a 633 nm laser at 613 μW power. Under these conditions the degradation of PbO_2 and other lower valence lead oxide phases is unlikely to occur.[43] The Raman spectra for crystalline reference compounds are provided in SI Figure S5. For β-PbO_2, characteristic peaks appear at 147, 286, and 337 cm^{-1} and are attributed to the vibrational stretching of Pb−O bonds.[43,44,46,47]

The Raman spectra obtained for the solid phases collected during dissolution are shown in Figure 5, together with the spectra obtained for crystalline massicot (β-PbO) and β-PbO_2. The Raman spectra for pure β-PbO and β-PbO_2 show similar profiles; the main peak for β-PbO appears at 140 cm^{-1} and that for β-PbO_2 at 147 cm^{-1}. For the samples collected during dissolution the main peaks appear between 138 and 140 cm^{-1} (Figure 5). This observation is consistent with the fact that oxygen vacancies and Pb^{2+} coexist in crystalline β-PbO_2. PbO_2 is known to be an extremely weak light scatterer because of its intrinsic ability to strongly absorb light and associated fluorescence phenomena.[43,44,48] Compared with PbO_2, lead(II) oxides give a more intense Raman signal. Thus, it is plausible to assume that the spectral features observed at 147, 286, and 337 cm^{-1} reflect the presence of Pb(II)−O rather than Pb(IV)−O, as Raman scattering by Pb^{2+} overwhelms the Pb^{4+} signal. This is consistent with our earlier calculations which indicate that >6% of the total lead content in the β-PbO_2 samples is present as Pb^{2+}.

The characteristic peak in the spectra shifted from 147 cm^{-1} (β-PbO_2) to 138 cm^{-1} at 20 min and to 136 cm^{-1} at 10 days (Figure 5). These shifts indicate a weakening in the bond strength of the Pb(II)−O moiety in the solid. At 90 days, this peak shifted back to 140 cm^{-1}, the same position as the characteristic peak of PbO and also of α-PbO_2 (Figure 5). This indicates after 90 days the Pb(II)−O bonds in the aging β-PbO_2 sample tended to be organized similarly to those in β-PbO or α-PbO_2. It is worth noting that Raman signals around 1045 cm^{-1}, which indicate C−O symmetric stretching of carbonates,[47] were not observed, suggesting that lead carbonates were not formed during the experiment. The Raman results thus indicate either that the Pb(II)−O defects in the crystal structure are changing or that a phase transformation (β- to α-PbO_2) is taking place due to oxidation by chlorine through the dissolution experiment.

X-ray Diffraction. XRD was used to characterize the solid samples collected durng dissolution (Figure 6). Pure β-PbO_2

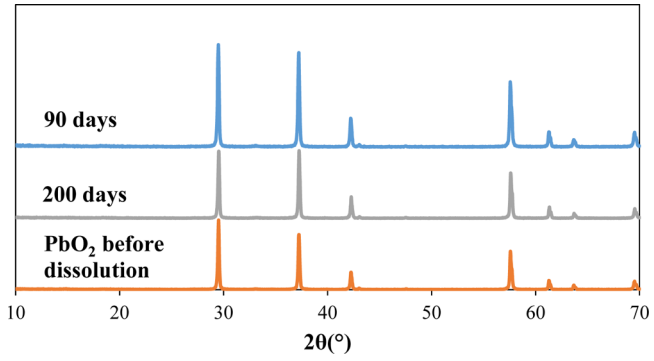

Figure 6. XRD patterns obtained on solids collected during dissolution experiments with a nominal initial free chlorine concentration of 2.5 mg Cl_2/L.

shows characteristic diffraction peaks at 29.6°, 37.4°, and 57.7°.[48] No characteristic peak shift or new peaks were observed in the diffractogram even after 200 days, indicating that β-PbO_2 is the only crystalline phase through the dissolution experiment.

Proposed Dissolution Mechanism. The solid phase analysis indicates that the dominant crystalline phase through the dissolution experiment is β-PbO_2. As observed by XRD, this

dx.doi.org/10.1021/es502133k | Environ. Sci. Technol. 2014, 48, 12525−12532

phase did not transform to another crystalline phase. However, the shift in the peak position in the Raman spectra suggests that, at the molecular level, the Pb−O bond structure in the crystal changes over time. The NIR spectra of samples collected from experiments with initial 2.5 and 5.0 mg/L as Cl_2 are the most informative (SI Figure S2). For both experiments, the shift in the NIR peak position and the associated changes in average oxidation state of the Pb in PbO_2 directly followed the consumption of free chlorine. This result suggests that the driving force for these changes is the amount of oxidant consumed over time rather than the absolute value of initial oxidant available. It is expected that further changes in the electronic structure of β-PbO_2 would occur over time if more initial chlorine was available for consumption. Whereas the NIR peaks of samples gathered from experiments with initial chlorine illustrated a bathochromic shift, aging samples collected from the control test (no chlorine) showed an opposite shift in the NIR peak position. This hypochromic shift suggests an increase in Pb^{2+} species in the solid, likely resulting from reduction of PbO_2 by water. This observation thus supports our hypothesis on consumption of free chlorine regulating the changes to the electronic structure of β-PbO_2.

A Pb(IV) oxide phase with a different electronic structure from that of the initial β-PbO_2 phase likely formed on the surface of the solid matrix, controlling the dissolution of lead into the aqueous phase over time. This new form of the solid phase has a relatively lower solubility than the initial β-PbO_2 phase as observed when chlorine was completely depleted and water was the only available reductant. The presence of this surface phase also explains why dissolved lead concentrations in experiment with initial 2.5 mg/L as Cl_2 were lower than in the control test (no chlorine), despite the higher ORP values observed in the control test. Although these ORP measurements can qualitatively describe aqueous conditions, they are not reliable for quantitative analysis of the speciation of redox couples.[49,50] Additionally, measured ORP values cannot be directly linked to pe-pH diagrams unless thermodynamic equilibrium is reached in the aqueous phase.[49,51] On the other hand, the different final dissolved lead levels between the control test and experiments indicate that free chlorine changed the morphology of the β-PbO_2 phase to a more stable structure. This further suggests that the changes in the structure of β-PbO_2 control the solubility of this phase and not the ORP conditions. The morphological changes that took place in the solid PbO_2 phase are the main reason for which much lower dissolved lead concentrations were observed in our experiments, compared with prior experiments[10,24,52] conducted without free chlorine.

Environmental Implications. Lead corrosion scales present in the pipe inner walls are oxidized continuously by residual chlorine over decades as residual chlorine is maintained in DWDS to provide disinfection for the safety of drinking water. Altough the composition and structure of scales are complex and vary depending on local conditions,[2,53,54] previous studies[1,3,4,19] reported that PbO_2 was the major lead-bearing solid phase in the surface layer of scales in some DWDS when free chlorine was used as disinfectant. PbO_2 solid phases present in the surface layer of the scales most likely have a different structure from that of commercially available plattnerite, and thus our observations might not be directly applied to changes in composition of actual field scale.[55] Our results, however, suggest that for the case of PbO_2-rich corrosion scale the dissolved lead concentrations should remain low, below actionable level (10 μg/L), if ORP decreases such as when residual chlorine is depleted. In contrast, higher dissolved lead concentrations have been consistently reported for DWDS that switched disinfectant from free chlorine to monochloramine (with an associated net decrease of ORP), even though PbO_2 was found uniformly layered on the surface of the corrosion scale.[3,18] Prior research has attributed these higher dissolved lead concentrations to the reduction of PbO_2 triggered by the decomposition of monochloramine[10,24] or to low ORP levels associated with the use of chloramines.[15,17] Our result shows that PbO_2 is still stable under low ORP levels after chlorine depletion. This therefore confirms previous studies linking the dissolution of PbO_2 after disinfectant switch to the decomposition of monochloramine to ammonia, ammonium, chloride, nitrogen, or unidentified intermediate species.[24,56,57] In contrast to our experimental conditions, various ions (chloride, sulfate, carbonates, nitrate, etc.) and reductants naturally present in drinking water in DWDS, such as NOM and Br^-, may be able to accelerate the reduction of this more stable PbO_2 phase and transform it into more soluble Pb(II) solids.[10,52,58] Although our experimental conditions are a simplification of actual field systems, our results clearly indicate the need for more research on the effects of decomposition of monochloramine and the presence of reductants such as NOM on the electronic structure of PbO_2 to clearly establish a mechanism for the dissolution of PbO_2 species under field drinking water conditions.

■ ASSOCIATED CONTENT

Supporting Information

Detailed experimental methodology together with the NIR spectra of the solid samples collected during dissolution experiments. This material is available free of charge via the Internet at http://pubs.acs.org.

■ AUTHOR INFORMATION

Corresponding Author

*(J.E.H.) Phone: (519) 661-2111, ext. 81262. E-mail: jherrer3@uwo.ca.

Notes

The authors declare no competing financial interest.

■ ACKNOWLEDGMENTS

Funding for this research was partially provided by the Canadian Water Network, the Corporation of the City of London, and the Canadian Foundation for Innovation. We acknowledge Prof. Daniel Resasco and his group at the University of Oklahoma for providing us access to their Raman spectroscopy facilities. The authors appreciate the comments and suggestions from the three anonymous reviewers as well.

■ REFERENCES

(1) Schock, M. R.; Harmon, S. M.; Swertfeger, J.; Lohmann, R. Tetravalent lead: a hitherto unrecognized control of tap water lead contamination. In *Proceedings AWWA Water Quality Technology Conference*, Nashville, TN, USA, Nov 2001; 2001; pp 11−15.

(2) Kim, E. J.; Herrera, J. E. Characteristics of lead corrosion scales formed during drinking water distribution and their potential influence on the release of lead and other contaminants. *Environ. Sci. Technol.* **2010**, *44* (16), 6054−6061.

(3) Schock, M. R.; Giani, R. Oxidant/disinfectant chemistry and impacts on lead corrosion. In *Proceedings of 2004 American Water Works Association Water Quality and Technology Conference*, 2004.

(4) Schock, M. R.; Scheckel, K.; DeSantis, M.; Gerke, T. L. Mode of occurrence, treatment, and monitoring significance of tetravalent lead. In *Proceedings AWWA Water Quality Technology Conference*, Quebec City, Quebec, Canada, 2005.
(5) Liu, H.; Korshin, G. V.; Ferguson, J. F. Investigation of the kinetics and mechanisms of the oxidation of cerussite and hydrocerussite by chlorine. *Environ. Sci. Technol.* **2008**, *42* (9), 3241−3247.
(6) Lytle, D. A.; White, C.; Nadagouda, M. N.; Worrall, A. Crystal and morphological phase transformation of Pb(II) to Pb(IV) in chlorinated water. *J. Hazard. Mater.* **2009**, *165* (1), 1234−1238.
(7) Wang, Y.; Xie, Y.; Li, W.; Wang, Z.; Giammar, D. E. Formation of lead(IV) oxides from lead(II) compounds. *Environ. Sci. Technol.* **2010**, *44* (23), 8950−8956.
(8) Liu, H.; Korshin, G. V.; Ferguson, J. F. Interactions of Pb(II)/Pb(IV) solid phases with chlorine and their effects on lead release. *Environ. Sci. Technol.* **2009**, *43* (9), 3278−3284.
(9) Zhang, Y.; Lin, Y.-P. Determination of PbO_2 formation kinetics from the chlorination of Pb(II) carbonate solids via direct PbO_2 measurement. *Environ. Sci. Technol.* **2011**, *45* (6), 2338−2344.
(10) Lin, Y.; Valentine, R. L. Reduction of lead oxide (PbO_2) and release of Pb(II) in mixtures of natural organic matter, free chlorine and monochloramine. *Environ. Sci. Technol.* **2009**, *43* (10), 3872−3877.
(11) Lin, Y. P.; Valentine, R. L. Reductive dissolution of lead dioxide (PbO_2) in acidic bromide solution. *Environ. Sci. Technol.* **2010**, *44* (10), 3895−3900.
(12) Shi, Z.; Stone, A. T. PbO_2(s, plattnerite) reductive dissolution by aqueous manganous and ferrous ions. *Environ. Sci. Technol.* **2009**, *43* (10), 3596−3603.
(13) Wang, Y.; Wu, J.; Giammar, D. E. Kinetics of the reductive dissolution of lead(IV) oxide by iodide. *Environ. Sci. Technol.* **2012**, *46* (11), 5859−5866.
(14) Xie, Y.; Wang, Y.; Singhal, V.; Giammar, D. E. Effects of pH and carbonate concentration on dissolution rates of the lead corrosion product PbO_2. *Environ. Sci. Technol.* **2010**, *44* (3), 1093−1099.
(15) Xie, Y.; Wang, Y.; Giammar, D. E. Impact of chlorine disinfectants on dissolution of the lead corrosion product PbO_2. *Environ. Sci. Technol.* **2010**, *44* (18), 7082−7088.
(16) Schock, M. R.; Wagner, I.; Oliphant, R. The corrosion and solubility of lead in drinking water. In *Internal Corrosion of Water Distribution Systems*, 2nd ed.; AWWA Research Foundation/TZW: Denver, CO, USA, 1996; pp 131−230.
(17) Switzer, J. A.; Rajasekharan, V. V.; Boonsalee, S.; Kulp, E. A.; Bohannan, E. W. Evidence that monochloramine disinfectant could lead to elevated Pb levels in drinking water. *Environ. Sci. Technol.* **2006**, *40* (10), 3384−3387.
(18) Edwards, M.; Dudi, A. Role of chlorine and chloramine in corrosion of lead-bearing plumbing materials. *J. Am. Water Works Ass.* **2004**, *96* (10), 69−81.
(19) Renner, R. Plumbing the depths of DC's drinking water crisis. *Environ. Sci. Technol.* **2004**, *38* (12), 224A−227A.
(20) Lytle, D. A.; Schock, M. R. Formation of Pb(IV) oxides in chlorinated water. *J. Am. Water Works Assoc.* **2005**, *97* (11), 102−114.
(21) Bagshaw, N. E.; Clarke, R. L.; Halliwell, B. The preparation of lead dioxide for X-ray diffraction studies. *J. Appl. Chem.* **1966**, *16* (6), 180−184.
(22) Li, X. H.; Pletcher, D.; Walsh, F. C. Electrodeposited lead dioxide coatings. *Chem. Soc. Rev.* **2011**, *40* (7), 3879−3894.
(23) Wang, Y.; Xie, Y.; Giammar, D. E. *Lead(IV) Oxide Formation and Stability in Drinking Water Distribution Systems*, 4211; Water Research Foundation: Denver, CO, USA, 2012.
(24) Lin, Y.; Valentine, R. L. Release of Pb(II) from monochloramine-mediated reduction of lead oxide (PbO_2). *Environ. Sci. Technol.* **2008**, *42* (24), 9137−9143.
(25) Copeland, A.; Lytle, D. A. Measuring the oxidation-reduction potential of important oxidants in drinking water. *J. Am. Water Works Assoc.* **2014**, *106* (1), 10−20.
(26) James, C.; Copeland, R.; Lytle, D. Relationships between oxidation-reduction potential, oxidant, and pH in drinking water. In *Proceedings of the AWWA Water Quality Technology Conference*, 2004; pp 14−18.
(27) Schüring, J. *Redox: Fundamentals, Processes and Applications*; Springer: Berlin, Germany, 2000.
(28) Bricker, O. P. Redox potential: its measurement and importance in water systems. In *Water Analysis: Inorganic Species, Part 1*; Minear, R. A., Ed.; Academic Press: New York, 1982.
(29) Galster, H. Technique of measurement, electrode processes and electrode treatment. In *Redox: Fundamentals, Processes and Applications*; Schüring, J., Schulz, H. D., Fischer, W. R., Böttcher, J., Duijnisveld, W. H. M., Eds.; Springer: Berlin, Germany, 2000; pp 13−23.
(30) Aly, S. A.; Kaid, M. A.; El-Sayed, N. Z. Some optical aspects of thermally evaporated lead oxide thin films. *Acta Phys. Polym., A* **2013**, *124* (4), 713−716.
(31) Lappe, F. Some physical properties of sputtered PbO_2 films. *J. Phys. Chem. Solids* **1962**, *23* (11), 1563−1566.
(32) Salagram, M.; Krishna Prasad, V.; Subrahmanyam, K. Optical band gap studies on xPb_3O_4−$(1-x)$ P_2O_5 lead[(II, IV)] phosphate glasses. *Opt. Mater.* **2002**, *18* (4), 367−372.
(33) Salagram, M.; Prasad, V. K.; Subrahmanyam, K. IR and optical study of Pb_3O_4 ($2PbO.PbO_2$) glass containing a small amount of silica. *J. Alloys Compd.* **2002**, *335* (1), 228−232.
(34) Scanlon, D. O.; Kehoe, A. B.; Watson, G. W.; Jones, M. O.; David, W. I. F.; Payne, D. J.; Egdell, R. G.; Edwards, P. P.; Walsh, A. Nature of the band gap and origin of the conductivity of PbO_2 revealed by theory and experiment. *Phys. Rev. Lett.* **2011**, *107* (24), No. 246402.
(35) Walsh, A.; Kehoe, A. B.; Temple, D. J.; Watson, G. W.; Scanlon, D. O. PbO_2: from semi-metal to transparent conducting oxide by defect chemistry control. *Chem. Commun.* **2013**, *49* (5), 448−450.
(36) Keester, K. L.; White, W. B. Electronic spectra of the oxides of lead and of some ternary lead oxide compounds. *Mater. Res. Bull.* **1969**, *4* (10), 757−764.
(37) Payne, D. J.; Paolicelli, G.; Offi, F.; Panaccione, G.; Lacovig, P.; Beamson, G.; Fondacaro, A.; Monaco, G.; Vanko, G.; Egdell, R. G. A study of core and valence levels in β-PbO_2 by hard X-ray photoemission. *J. Electron Spectrosc. Relat. Phenom.* **2009**, *169* (1), 26−34.
(38) Davis, E. A.; Mott, N. F. Conduction in non-crystalline systems V. Conductivity, optical absorption and photoconductivity in amorphous semiconductors. *Philos. Mag.* **1970**, *22* (179), 0903−0922.
(39) Hossein, A. A.; Hogarth, C. A.; Beynon, J. Optical absorption in CeO_2-V_2O_5 evaporated thin films. *J. Mater. Sci. Lett.* **1994**, *13* (15), 1144−1145.
(40) Khan, G. A.; Hogarth, C. A. Optical absorption spectra of evaporated V_2O_5 and co-evaporated V_2O_5/B_2O_3 thin films. *J. Mater. Sci.* **1991**, *26* (2), 412−416.
(41) Wang, Y.; Wu, J.; Wang, Z.; Terenyi, A.; Giammar, D. E. Kinetics of lead(IV) oxide (PbO_2) reductive dissolution: role of lead(II) adsorption and surface speciation. *J. Colloid Interface Sci.* **2013**, *389* (1), 236−243.
(42) Izvozchikov, V. A. Crystallochemical peculiarities and shape of the absorption edge of lead oxides. *Phys. Status Solidi A* **1972**, *14* (1), 161−170.
(43) Burgio, L.; Clark, R. J.; Firth, S. Raman spectroscopy as a means for the identification of plattnerite (PbO_2), of lead pigments and of their degradation products. *Analyst* **2001**, *126* (2), 222−227.
(44) Black, L.; Allen, G. C.; Frost, P. C. Quantification of Raman spectra for the primary atmospheric corrosion products of lead. *Appl. Spectrosc.* **1995**, *49* (9), 1299−1304.
(45) Aze, S.; Delaporte, P.; Vallet, J. M.; Detalle, V.; Grauby, O.; Baronnet, A. Towards the restoration of darkened red lead containing mural paintings: a preliminary study of the β-PbO_2 to Pb_3O_4 reversion by laser irradiation. In *Lasers in the Conservation of Artworks: Proceedings of the International Conference Lacona VII*, Madrid, Spain, Sept 17−21 2007; CRC Press: Boca Raton, FL, USA, 2008; p 11.
(46) Trettenhahn, G. L. J.; Nauer, G. E.; Neckel, A. Vibrational spectroscopy on the PbO-$PbSO_4$ system and some related

compounds: Part 1. Fundamentals, infrared and Raman spectroscopy. *Vib. Spectrosc.* **1993**, *5* (1), 85−100.
(47) Ciomartan, D. A.; Clark, R. J. H.; McDonald, L. J.; Odlyha, M. Studies on the thermal decomposition of basic lead(II) carbonate by Fourier-transform Raman spectroscopy, X-ray diffraction and thermal analysis. *J. Chem. Soc., Dalton Trans.* **1996**, *18*, 3639−3645.
(48) Bullock, K. R.; Trischan, G. M.; Burrow, R. G. Photoelectrochemical and microprobe laser Raman studies of lead corrosion in sulfuric acid. *J. Electrochem. Soc.* **1983**, *130* (6), 1283−1289.
(49) Peiffer, S. Characterisation of the redox state of aqueous systems: towards a problem-oriented approach. In *Redox: Fundamentals, Processes And Applications*; Springer: Berlin, Germany, 2000; pp 24−41.
(50) Sigg, L. Redox potential measurements in natural waters: significance, concepts, and problems. In *Redox: Fundamentals, Processes and Applications*; Schüring, J., Schulz, H. D., Fischer, W. R., Böttcher, J., Duijnisveld, W. H. M., Eds.; Springer: Berlin, Germany, 2000; pp 1−12.
(51) Linberg, R. D.; Runnels, D. D. Ground water redox reactions: an analysis of equilibrium state applied to Eh measurements and geochemical modeling. *Science* **1984**, *225* (1665), 925−927.
(52) Lin, Y.; Valentine, R. L. The release of lead from the reduction of lead oxide (PbO_2) by natural organic matter. *Environ. Sci. Technol.* **2008**, *42* (3), 760−765.
(53) Kim, E. J.; Herrera, J. E.; Huggins, D.; Braam, J.; Koshowski, S. Effect of pH on the concentrations of lead and trace contaminants in drinking water: a combined batch, pipe loop and sentinel home study. *Water Res.* **2011**, *45* (9), 2763−2774.
(54) Schock, M. R.; Hyland, R. N.; Welch, M. M. Occurrence of contaminant accumulation in lead pipe scales from domestic drinking-water distribution systems. *Environ. Sci. Technol.* **2008**, *42* (12), 4285−4291.
(55) Dryer, D. J.; Korshin, G. V. Investigation of the reduction of lead dioxide by natural organic matter. *Environ. Sci. Technol.* **2007**, *41* (15), 5510−5514.
(56) Vikesland, P. J.; Ozekin, K.; Valentine, R. L. Monochloramine decay in model and distribution system waters. *Water Res.* **2001**, *35* (7), 1766−1776.
(57) Valentine, R. L.; Jafvert, C. T. General acid catalysis of monochloramine disproportionation. *Environ. Sci. Technol.* **1988**, *22* (6), 691−696.
(58) Zhang, Y.; Lin, Y.-P. Elevated Pb(II) release from the reduction of Pb(IV) corrosion product PbO_2 induced by bromide-catalyzed monochloramine decomposition. *Environ. Sci. Technol.* **2013**, *47* (19), 10931−10938.